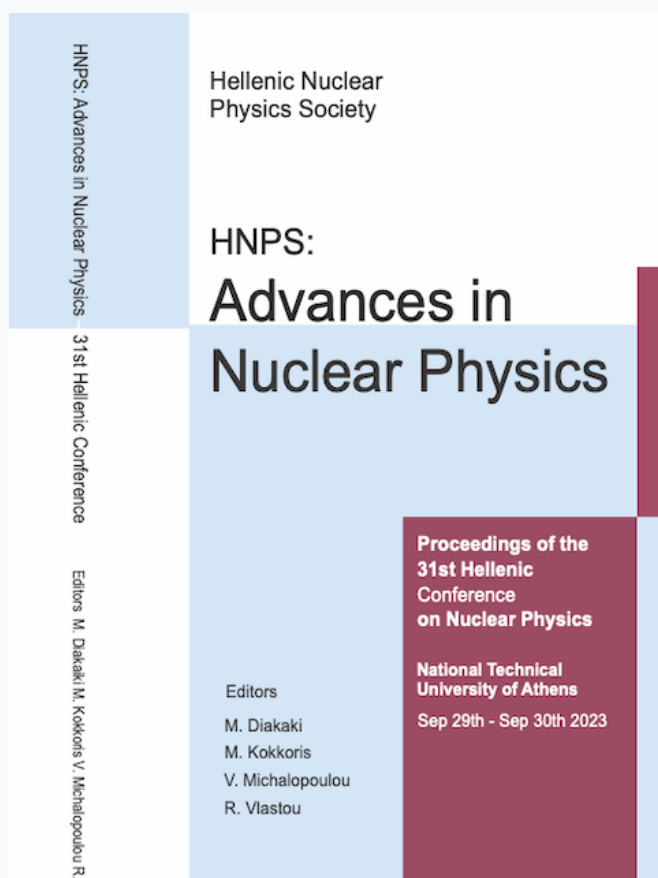


# HNPS Advances in Nuclear Physics

Vol 30 (2024)

HNPS2023



## **αSPECT: Adaptation of existing radon detectors to deep-sea operation**

*Ioannis Madesis, Varvara Lagaki, Georgios Siltzovalis, Theo J. Mertzimekis*

doi: [10.12681/hnpsanp.6219](https://doi.org/10.12681/hnpsanp.6219)

Copyright © 2024, Ioannis Madesis, Varvara Lagaki, Georgios Siltzovalis, Theo J. Mertzimekis



This work is licensed under a [Creative Commons Attribution-NonCommercial-NoDerivatives 4.0](https://creativecommons.org/licenses/by-nc-nd/4.0/).

### To cite this article:

Madesis, I., Lagaki, V., Siltzovalis, G., & Mertzimekis, T. J. (2024). αSPECT: Adaptation of existing radon detectors to deep-sea operation. *HNPS Advances in Nuclear Physics*, 30, 131–136. <https://doi.org/10.12681/hnpsanp.6219>

# **$\alpha$ SPECT: Adaptation of existing radon detectors to deep-sea operation\***

I. Madesis\*, V. Lagaki, G. Siltzovialis, T.J. Mertzimekis

*Department of Physics, National and Kapodistrian University of Athens, 15784, Athens, Greece*

**Abstract** Among the naturally occurring radioactive materials (NORM), radon and its isotopes  $^{222}\text{Rn}$  and  $^{220}\text{Rn}$ , being the only gaseous products, have a significant role due to their unique transport properties and common chemical characteristics within the respective decay chains of uranium and thorium. Continuous monitoring of radon emissions has diverse applications in geosciences, including the potential for earthquake precursors and their association with changes in volcanic activity [1]. In this work, we report on the development, testing, and characterization of a one-of-a-kind and innovative alpha radiation spectrometer known as  $\alpha$ SPECT. RAMONES [2], a project funded by the EU H2020 FET Proactive program, aims to develop prototype instruments for continuous and in situ measurements of radioactivity, both natural and artificial, in the marine environment. These instruments will be deployed on a stationary benthic laboratory or on autonomous underwater gliders (AUG). This instrument, specifically designed for operation in the deep sea, will be hosted on the benthic laboratory. To ensure the suitability of  $\alpha$ SPECT for deep-sea environments, the detector design is adapted to commercial cylindrical enclosures capable of withstanding harsh marine conditions. Through the deployment of  $\alpha$ SPECT, we anticipate gaining insight into deep-sea geochemical processes related to radon emission and circulation. This includes the investigation of sediment-water interactions, water volume dynamics, and properties of submarine hydrothermal vents. Currently,  $\alpha$ SPECT is undergoing development, and initial testing is scheduled to commence soon.

**Keywords** radon detection, continuous monitoring, hydrothermal vent field, marine radioactivity

## **INTRODUCTION**

Radioactivity monitoring radioactivity in the marine environment poses significant challenges due to the harsh ocean conditions and the obstacles encountered during detection caused by water attenuation. The RAMONES (RADioactivity Monitoring in Ocean EcosystemS) [2] project is a bold FET Proactive Research Programme with the goal of surpassing current constraints such as measurement duration. It aims to offer in situ, near-real-time, and long-term radioactivity monitoring in the most distant and inhospitable aquatic environments. To achieve this, a pioneering fleet of underwater radioactivity sensors is currently under development and in the testing phase for both mobile autonomous underwater gliders, and a stationary benthic laboratory.

One of the instruments placed on the stationary benthic laboratory is  $\alpha$ Spect.  $\alpha$ Spect is a custom radon detector, with a modified shape, adapted to underwater housings. The detection method that has been chosen is electrostatic precipitation of the radon decay product. By modifying the shape and size of the precipitation chamber, sensitivity comparable to commercial models, can be achieved. The goal of  $\alpha$ Spect is to not only monitor radon concentration variations within the marine environment, but also to quantify radon content. The  $\alpha$ SPECT radon detector consists of essentially three modules: The gas extraction module, the detector module, and the battery module. Here, we primarily focus on the detector module.  $\alpha$ SPECT is currently under development and the next sections describe the production stages of the detector module to some extent.

---

\* Corresponding author: [imadesis@phys.uoa.gr](mailto:imadesis@phys.uoa.gr)

## EXPERIMENTAL DETAILS

The method employed for radon detection is electrostatic precipitation. In this method, the gas mixture, extracted from water, is guided inside a conducting chamber. The various steps of this process are presented in Figure 1. The water is circulated with the use of a water pump, through a contaminant filter and a gas extracting membrane. The gaseous sample is filtered for  $\text{CO}_2$  and humidity and guided towards the precipitation chamber. This chamber has positively charged walls and a ground biased particle detector. Once the introduced radon alpha decays to the respective polonium isotope, there is a 88% [3] probability of the daughter isotope to be positively charged. Hence, the electrostatic field deposits the polonium ion onto the particle detector, where there is a 50% detection probability (due to the geometrical factor) of the subsequent alpha decay of polonium to the respective lead isotopes, along with the rest daughter product decays. See Figure 2 for a graphic description.

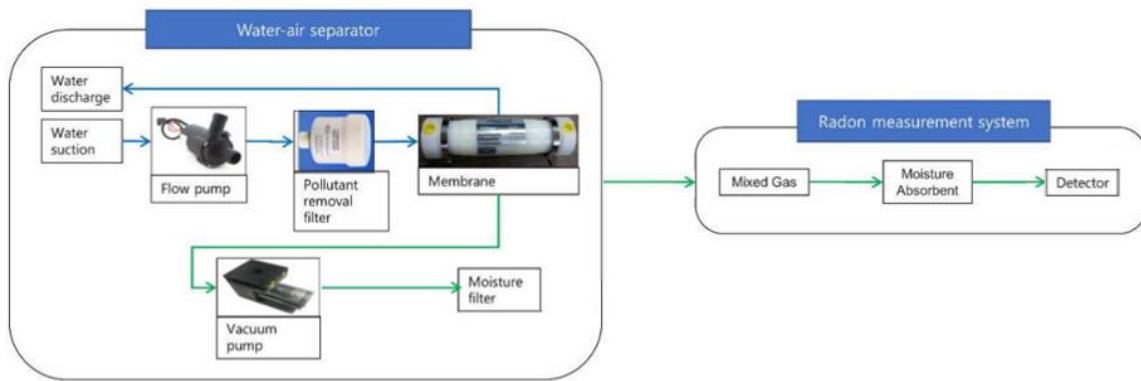


**Figure 1.** Various stages for the air sample extraction from water and purification as exhibited in Ref. [4]. The water is circulated within a closed loop, and a gaseous sample is extracted with the use of a membrane. With the use of a vacuum pump the sample is driven through filters for purification.

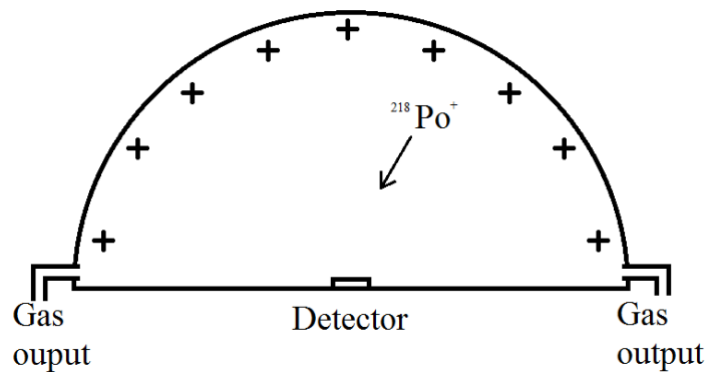


**Figure 2.** Rough outline of the principle of operation for  $\alpha$ SPECT. The gaseous sample enters the precipitation chamber. Singly charged polonium, as the decay product of radon, precipitates onto the detector. See text for more details.

The main advantage of this technique is the elimination from the alpha spectrum of the lines at 5.49 and 5.29 MeV that belong to  $^{222}\text{Rn}$  and  $^{220}\text{Rn}$ , respectively. Since the energies of the alpha particles of the alpha emitting radon daughters (Po-218,214,210,216,212) differ significantly, including both decay chains, this technique allows for a clear spectrum, with no line overlapping, therefore, much easier to interpret. More precisely, said differences of the energies of the alphas emitted from the daughters are in average approximately 0.8 MeV, thus no high-resolution particle detector is required.

For this instrument, a silicon particle detector, similar to the one used in [5] was chosen.

The sensitivity of this type of sensors is proportional, among others, to the sampling volume [6]. Specifically, as seen in Eqn. 1 from Ref. [6] slightly transformed, the Calibration Factor ( $C.F.$ ), which is inversely proportional to sensitivity, is inversely proportional to the sampling volume:

$$C.F. = \frac{1}{V \times r_+ \times \varepsilon_p \times e_a \times 60[sec]} \quad (1)$$

where  $V$  is the sampling volume,  $r_+$  is the probability of the emanated polonium isotope to be positively charged,  $\varepsilon_p$  is the collection efficiency of the precipitation chamber,  $e_a$  is the efficiency of the  $\alpha$  particle detector. Therefore, to maximize the efficiency of  $\alpha$ SPECT, we need to maximize the sampling volume. The first design iterations towards this goal can be seen in Fig. 3.

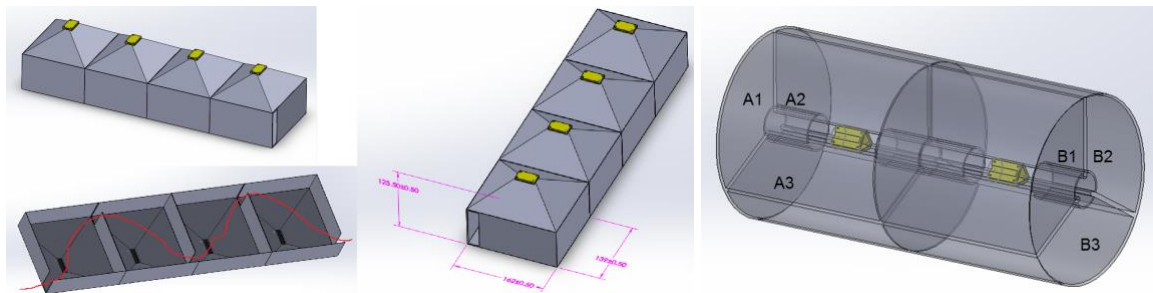


**Figure 3.** (Left) Combination of multiple detection volumes in one instrument. (Right) Adaptation of the first design to a cylindrical underwater housing typically used for large sea depths.

The idea is that instead of having one large volume, that would require unreasonably high voltages [7], for underwater measurements, same sensitivity can be achieved by combining a few smaller sampling volumes. Four consecutive precipitation chambers are connected with the sample gas passing in series in order to avoid stale gas between measurements. It should be noted that the hemispherical geometry, typically used for such detectors was converted to a quasi-hemispherical one, to utilize maximum volume. However, instruments intended to operate in deep sea environment are constrained by cylindrical housings, designed to withstand the large pressures (1 atm/10 m depth) that characterize such environments.

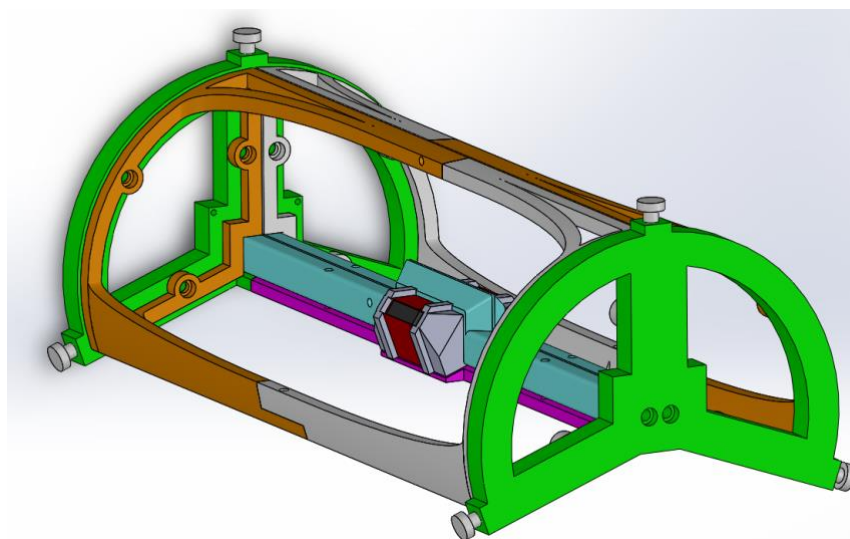


**Figure 4.**  $\alpha$ Spect detection module final CAD design. See text for details.

Considering that the maximization of sensitivity requires the full utilization of the available volume, a new detector geometry was proposed, shown in Fig. 3 (Right). In this version, the hemispherical geometry typically used in this technique, is now converted to 120° cylindrical sections. Again, the path of the sample gas is required to pass through all the chambers, however, this design the input and output gas can either be on the same or opposite end caps. However, this design, while ideal in some respects, can be rather problematic in others such as the increased distance between the preamplifier and the detector.

In Fig. 4, the final design for  $\alpha$ SPECT is presented. Instead of utilizing three equal spaces per cylinder, the volume is divided into two 110°, equal detection volumes, while the rest 140° is reserved for two preamplifiers, and an analogue adder sending a single signal to a Multi-Channel Analyzer (MCA) unit. This version is designed for a 6" underwater housing. The majority of the inner conducting surfaces is replaced with a metallic mesh that allows for free air flow and minimizes the probability of stale gas left within. The parts are designed with respect to  $C_{2v}$  symmetry to reduce the complexity, and be 3D-printable.

**Table 1.** Module dimensions along with sensitivity calculations

Module Dimensions		Sensor Sensitivity	
Degrees	110	Positively charged emanated $^{218}\text{Po}$ ( $r_+$ )	88%
Radius (dm)	0.762	Collection efficiency ( $\epsilon_p$ )	75%
Length (dm)	3	$\alpha$ -particle detection eff. (<50%) ( $\epsilon_\alpha$ )	40%
Module Volume (L)	1.50	Calibration Factor C.F. ( $\text{Bq/m}^3/\text{cpm}$ )	20.97
Total sensor volume (L)	3.01	Sensitivity ( $10^{-2} \text{ cpm/Bq/m}^3$ )	4.77
		Sensitivity ( $\text{cpm/kBq/m}^3$ )	47.68

In Table 1 the main dimensions of the detector are presented that provide a sampling volume of approximately three liters (3 L), a 4-fold volume, when compared with commercially available, State of the Art detectors. Additionally, Table 1 includes calculations regarding its sensitivity with respect to the calculated volume. These calculations are based on Eqn. 1, by applying certain estimations. More specifically, a collection efficiency ( $\epsilon_p$ ) of approximately 75%, and a particle detection efficiency of 40% are some safe estimations regarding the instrument's performance, and the resulting efficiency is again, comparable to commercially available detectors.

## RESULTS AND DISCUSSION

In Fig. 5 the printed model is shown, preparing for the first test in an isolated environment with a  $^{226}\text{Ra}$  source. In close proximity to the detector there is the respective preamplifier, for single detector mode, and feedthroughs have been prepared for the High Voltage input, preamp power supply, and preamp output.

All the aforementioned equipment is mounted on the cap of an airtight, metallic container. Within the container, an unsealed  $^{226}\text{Ra}$  source will be placed, populating  $^{222}\text{Rn}$  daughters. The metallic container serves as a Faraday cage, while special care has been taken to avoid ground loops. More specifically, both the internal preamp and the external MCA have floating power supplies, and the high voltage power supply (HVPS) feedthrough does not include a ground connection. Therefore, the ground connectivity is "linear": For the initial tests, it starts from the oscilloscope to the preamp and then to the detector, while for the final setup with the MCA and the laptop, we avoided multiple ground connections per device to eliminate ground loops.





**Figure 5.** Experimental setup for initial tests. See text for more details.

**Table 2.** Details for all the detector components regarding mass, volume, along with printing times

Part	Mass (gr)	Fil. volume (cm <sup>3</sup> )	Printing Time (min)	Times Printed
Holder	8.46	6.82	93	x1
Dual side mesh support	14.94	12.05	139	x1
Endcap (short)	24.53	19.78	445	x2
Endcap (long)	26.92	21.07	480	x2
Endcap (base)	34.80	28.07	346	x2
Central mesh support	15.44	12.45	155	x2
<b>Total</b>	<b>226.78</b>	<b>181.61</b>	<b>3084</b>	<b>10</b>

The parts of the detector were designed in CAD software, and compatible for additive manufacturing. In Table 2 are few printing details. As it can be seen, the total mass of the parts is approximately 225 g, and it required a little less than 52 h of printing utilizing the 0.1 mm detail setting of the 3D printer.

## CONCLUSIONS

A novel detector for radon measurements in deep sea environments has been designed, assembled and is currently under characterization. It utilizes a custom precipitation chamber that allows for the distinction of  $^{222}\text{Rn}$  and  $^{220}\text{Rn}$ , the two most abundant radon isotopes. The precipitation chamber is designed to be placed in suitable housings for deep sea operation. This design is based on additive manufacturing, and allows for sampling volumes, and therefore sensitivities much higher than commercially available detectors. The next steps aim at testing  $\alpha\text{SPECT}$ , including qualitative measurements for energy calibration, along with quantitative measurements for efficiency calculations using a calibrated radon detector.

## Acknowledgments

This work is supported by European Union under Horizon 2020 FET Proactive Programme via grant agreement No. 101017808



## References

- [1] S.M. Barbosa et al., *Eur. Phys. J. ST* 224, 597 (2015), doi: 10.1140/epjst/e2015-02393-y
- [2] T.J. Mertzimekis et al., *Proc. GoodIT 2021*, 216 (2021), doi: 10.1145/3462203.3475906
- [3] P.K. Hopke, *Env. Int.*, 15, 299, (1989), doi: 10.1016/0160-4120(89)90042-1
- [4] C.W. Lee et al., *Rad. Meas.* 121, 54 (2019), doi: 10.1016/j.radmeas.2018.11.006
- [5] T. Beck et al., *NIM A* 951, 163090 (2020), doi: 10.1016/j.nima.2019.163090
- [6] M.C. Chu et al., *NIM A* 808, 156 (2016), doi: 10.1016/j.nima.2015.11.093
- [7] C. Mitsuda et al., *NIM A* 497, 414 (2003), doi: 10.1016/S0168-9002(02)01923-X